We would like to thank the community for the invaluable comments and suggestions. Here are our responses to the community's comments.

The methods and experimental setup section would benefit from additional details. The specific implementation of the retrieval method is unclear and should be elaborated. Moreover, the method of statistical background error covariance needs further explanation. The experimental procedures for the two case studies also need to be described in greater detail.

Reply: Thanks for the valuable comments. Added as "WRF v4.3 and its data assimilation system WRFDA v4.3 are used in this study. Two convective cases are studied in the study: 14 June in 2020 (called Case 1; Fig. 1a) and 6 August in 2018 (denoted as Case 2; Fig. 1b). For case 1, the model domain contains 500×471 with a 3 km horizontal grid spacing, and 50 vertical levels. For case 2, the model domain contains 723 × 691 with a 3 km horizontal grid spacing, and 50 vertical levels. The specific applications of physical parametrizations are as follows: the WRF Double-Moment 6-Class Microphysics (WDM6) scheme, the Rapid Radiative Transfer Model (RRTM) long wave radiation scheme (Mlawer et al., 1997), the Dudhia short-wave radiation scheme (Dudhia, 1989), the Yonsei University (YSU) boundary layer scheme (Hong et al., 2006), and the Noah Land Surface Model (Chen and Dudhia, 2001) for land surface process scheme. No cumulus parameterization scheme is employed. As shown in Table 1, three data assimilation (DA) experiments are conducted to evaluate the effects of all retrieval methods in the study. For all three DA experiments, the initial and lateral boundary conditions are provided by the NCEP Global Forecast System (GFS) data. Besides, the specific flowchart is presented in the Fig. 2. The radar observations used in two cases undergo a series of preprocessing and quality control procedure, including anomaly detection, velocity de-aliasing, and so on. The observation errors of radar radial velocity and radar reflectivity are set to 2 m s^{-1} and 5 dBZ, respectively." in the section 3.

Minor points

1. It is a little bit confusing to use the "the positive impact is not promising" here.

Reply: Thanks for the valuable comments. It is revised as “However, due to the absence of ice phase particles, the scheme showed limited effectiveness in deep moist convection cases dominated by cold-cloud processes.”

2. It is recommended to include topographic information in the simulation domain map shown in Figure 1 to provide additional geographic context.

Reply: Thanks for the valuable comments. Fig.1 has been modified.

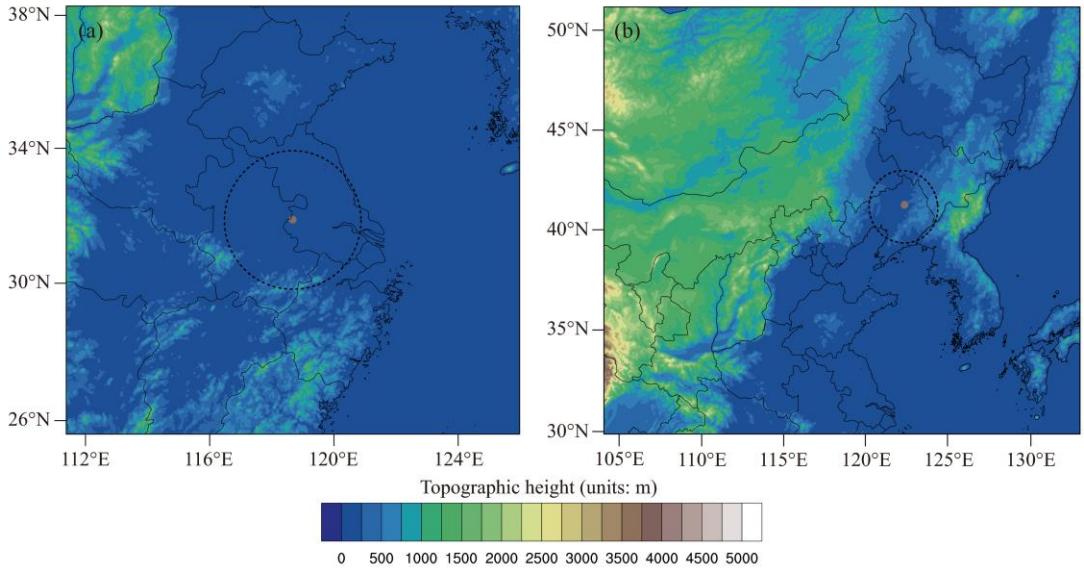

Fig. 1. The simulated area of (a) Case 1 and (b) Case 2, with the detecting ranges of the Nanjing radar and Shenyang Radar. Both radars are S-band Doppler radars with a maximum coverage range of 230 km. The radial velocity and reflectivity observations have range resolutions of 250 m and 1000 m, respectively.

3. More information about the radar observations used in the data assimilation should be provided, including details such as the type of radar, spatial and temporal resolution, quality control procedures.

Reply: Thanks for the valuable comments.

Added as “Besides, the specific flowchart is presented in the Fig. 2. The radar observations used in two cases undergo a series of preprocessing and quality control

procedure, including anomaly detection, velocity de-aliasing, and so on. The observation errors of radar radial velocity and radar reflectivity are set to 2 m s^{-1} and 5 dBZ, respectively." in the section 3.

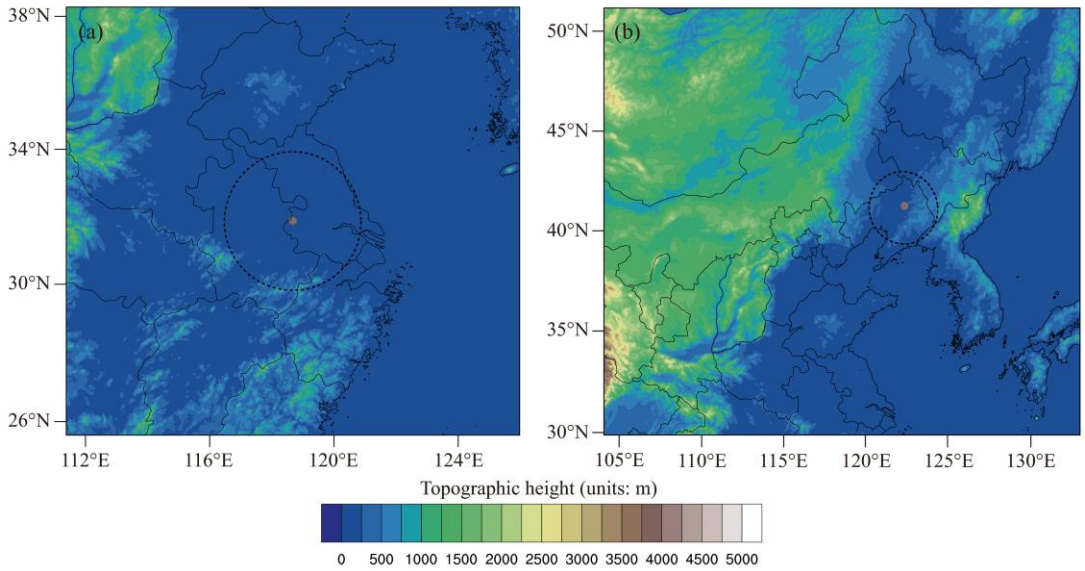

Fig. 1. The simulated area of (a) Case 1 and (b) Case 2, with the detecting ranges of the Nanjing radar and Shenyang Radar. Both radars are S-band Doppler radars with a maximum coverage range of 230 km. The radial velocity and reflectivity observations have range resolutions of 250 m and 1000 m, respectively.

4. The wind vector arrows in Figure 6 are difficult to discern clearly. Please consider adjusting the arrow color, thickness, or scale to enhance visibility against the background.

Reply: Thanks for the valuable comments. Fig. 6 has been modified.

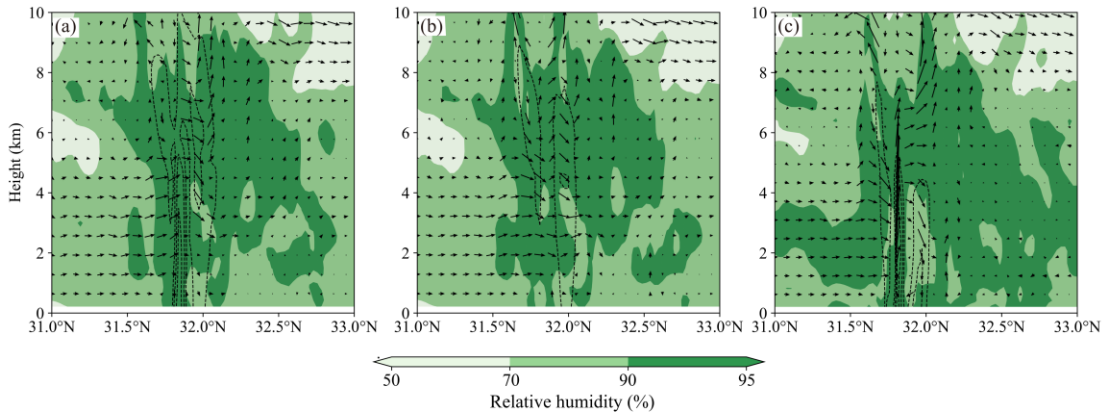

Fig. 6. The cross sections of relative humidity (shading; units: %), radar reflectivity (black contours starting at 40 dBZ; units: dBZ), and wind vectors for (a) EXP_temp, (b) EXP_bg and (c) EXP_temp-

bg along the line a1-a2. These are 1-hour forecasts initialized at 1501 UTC.

5. The description of the Equitable Threat Score (ETS) is incomplete. Please provide more details on the calculation method.

Reply: Thanks for the valuable comments.

Added as "In this paper, Equitable Threat Score (ETS) is used to quantitatively evaluate the forecast effect of heavy precipitation in each group of experiments. The specific calculation formula of ETS is as follows:

$$\mathrm{ETS} = \frac{\mathrm{A}-\mathrm{R}}{\mathrm{A}+\mathrm{B}+\mathrm{C}-\mathrm{R}}, \tag{13}$$

$$\mathrm{R} = \frac{(\mathrm{A}+\mathrm{C})\times(\mathrm{A}+\mathrm{B})}{\mathrm{A}+\mathrm{B}+\mathrm{C}+\mathrm{D}}, \tag{14}$$

where A, B, C, and D are the number of hits, the false alarms, the misses, and the correct negatives. The R means the probability to have a correct forecast by chance." in the section 4.1.

6. The discussion of θ behavior in convectively unstable environments aligns with theoretical expectations in the Figure 12. While this background is useful, the section could be condensed to focus more sharply on novel aspects of the study.

Reply: Thanks for the valuable comments. It is modified with "Fig. 12 displays the vertical cross sections of the pseudo-equivalent potential temperature (θse), wind components, and reflectivity at 2100 UTC for EXP_temp, EXP_bg, and EXP_temp-bg. All three data assimilation (DA) experiments exhibit a high-low-high vertical distribution of θse. It suggests that the vertical structure of the atmosphere is unstable in this region, with dry conditions prevailing in the upper levels and moist conditions in the lower levels. This type of vertical structure is favorable for the development of severe convective weather events. In the middle layer, there is a zone with relatively high θse value for EXP_bg and EXP_temp-bg. Specifically, a warm-core structure is identified near 123.85°N, accompanied by strong upward motion. This results in the release of unstable energy indicate that a severe convective system is continuously developing. Additionally, compared with EXP_bg, EXP_temp-bg yields a more extensive and deeper updraft column."